



Proposed Approaches for Brain Tumors Detection Techniques Using Convolutional Neural Networks

Somaya A. El-Feshawy^{1,*}, Waleed Saad², Mona Shokair³, and Moawad I. Dessouky⁴

Citation: El-Feshawy, S.; Saad, W.; Shokair, M.; Dessouky, M. *Inter. Jour. of Telecommunications, IJT* 2022, Vol. 02, Issue 01, pp. 1-14, January 2022. <https://ijt-adc.org/articles/2805-3044/165806>.

Editor-in-Chief: Yasser M. Madany.

Academic Editor: Youssef Fayad

Received: 2022-01-19.

Accepted: 2022-04-26.

Published: 2022-04-28.

Publisher's Note: The International Journal of Telecommunications, IJT, stays neutral regard-ing jurisdictional claims in published maps and institutional affiliations.



Copyright: © 2022 by the authors. Submitted for possible open access publication under the terms and conditions of the International Journal of Telecommunications, Air Defense College, ADC, (<https://ijt-adc.org>).

¹ Electronic and Electrical Communication Department, Faculty of Electronic Engineering, Menoufia University, Egypt, somaya.feshawy@gmail.com

² Electronic and Electrical Communication Department, Faculty of Electronic Engineering, Menoufia University, Egypt, Waleedsaad100@yahoo.com

³ Electronic and Electrical Communication Department, Faculty of Electronic Engineering, Menoufia University, Egypt, shokair_1999@hotmail.com

⁴ Electronic and Electrical Communication Department, Faculty of Electronic Engineering, Menoufia University, Egypt, dr_moawad@yahoo.com

* Correspondence: somaya.feshawy@gmail.com

Abstract: A brain tumor is an intracranial mass consisting of irregular growth of brain tissue cells. Medical imaging plays a vital role in discovering and examining the precise performance of organs. The performance of object detection has increased dramatically by taking advantage of recent advances in deep learning. This paper presents a Convolutional Neural Network (CNN) architecture model-based classification approach for brain tumor detection from Magnetic Resonance Imaging (MRI) images. The network training was carried out in both the original dataset and the augmented dataset. Whereas the whole brain MRI images were scaled to fit the input image size of each pre-trained CNN network. Moreover, a comparative study between the proposed model and other pre-trained models was made in terms of accuracy, precision, specificity, sensitivity, and F1-score. Finally, experimental results reveal that without data augmentation, the proposed approach achieves an overall accuracy rate of 96.35 percent for a split ratio of 80:20. While the addition of data augmentation boosted the accuracy to 97.78 percent for the same split ratio. Thus, the obtained results demonstrate the effectiveness of the proposed approach to assist professionals in Automated medical diagnostic services.

Keywords: Brain Tumor; MRI; Convolutional Neural Networks; Data Augmentation.

1. Introduction

A brain tumor is a mass inside the skull that consists of irregular growth of brain tissue cells. In general, the body helps cells to grow and divide, if this balance in cell division is disrupted, then a tumor may develop. Hence, any abnormal growth of body tissues is called a tumor. Which is either cancerous (malignant) or non-cancerous (benign). Benign tumors vary from malignant tumors in that they do not expand to other tissues and can be surgically removed [1]. A brain tumor is not as frequent as other malignancies such as breast cancer or lung cancer, yet it is nevertheless the tenth biggest cause of death worldwide. An estimated 25,050 persons (14,170 men and 10,880 women) will be diagnosed with primary malignant tumors of the brain and spinal cord in the United States this year [2]. Medical imaging has a vital role in detecting and examining the accurate functioning of organs. Magnetic Resonance Imaging (MRI) is considered the most important diagnostic method for brain tumors that aid in treatment arrangement. Because of the nature of the brain, detecting tumor areas in the brain is one of the most important topics. Object detection performance has substantially increased by utilizing recent advances in deep learning.

In the past few years, Machine Learning (ML) and Deep Learning (DL) have played a significant role in the early detection of tumors [3]. DL requires a large amount of data to be efficiently trained. The training process can be executed using Computed Tomography (CT) scan images or Magnetic Resonance Imaging (MRI) [4]. Data sets with lower sizes can be optimized using data augmentation. Flipping, translation, and gradient rotation are the most common methods [5]. Therefore, using a data augmentation methodology and a convolutional neural network model, a method for classifying brain tumors as cancerous or non-cancerous was developed. This paper presents a proposed CNN model for classifying brain tumors, in which a brain MRI dataset is used. Then, the result of the classification process will be compared to other models to determine which technique(s) are best suited for medical images. In addition, the effect of dataset augmentation will be made. The suggested model is used in scenarios where 80 percent or 70 percent of the data is used for training and 20 percent, or 30 percent of the data is used for testing. In the case of the original dataset and the dataset that was added to it. Finally, simulation programs will be implemented to analyze the proposed model performance and compare the result of the proposed models with pre-trained models.

The rest of the paper is designed as follows: In Section 2, the literature review will be presented. The proposed methodology will be illustrated in Section 3. In section 4, the simulation analysis will be introduced. Finally, the conclusions will be illustrated in Section 5.

2. Literature Review

Many studies have been conducted to classify and segment MRI pictures of the brain using deep learning. Basheera et al. [6], used a method for categorizing brain cancers Where the tumor is first segmented from the MRI picture and then the segmented fragment is extracted using a pre-trained convolutional neural network and random gradient descent. Carlo, Ricciardi, et al. [7] utilized multinomial logistic regression and the k-nearest neighbour techniques to categorize pituitary adenomas tumor MRIs. With an AUC curve of 98.4 percent, the technique obtained an accuracy of 83 percent on multinomial logistic regression and 92 percent on a k-nearest neighbour. Muhammad Sajjad et al. [8] proposed classifying multi-grade malignancies using a data augmentation technique on MRI images and then tweaking it with a pre-trained VGG-19 CNN Model. Sunanda Das et al., [9] presented an image processing technique to train a CNN model to identify distinct brain tumor types and achieved 94.39 percent accuracy with an average precision of 93.33 percent. Romeo, Valeria, et al., [10] used Naïve Bayes and k-nearest neighbour to predict tumor grades and nodal status from CT scans of primary tumor lesions and achieved the greatest accuracy of 92.9 percent. Muhammed Talo et al. [11] classified normal and pathological brain MRI images with 100 percent accuracy using the ResNet34 pre-trained CNN model, a transfer learning technique, and Data Augmentation. Arshia Rehman et al. [12] classified pituitary, glioma, and meningioma brain cancers using three different pre-trained CNN models (VGG16, AlexNet, and GoogleNet). During this Transfer learning approach, VGG16 achieves the best accuracy of 98.67%. Ahmet inar et al. [13] changed the pre-trained ResNet50 CNN model by eliminating its last 5 levels and replacing them with 8 new layers, then compared its accuracy to other pre-trained models such as GoogleNet, AlexNet, and ResNet50. The modified ResNet50 model performed well, reaching 97.2 percent accuracy. SVM was utilized to differentiate between malignant and benign cancers. A classification scheme based on a pre-trained neural network has been suggested, where MR im- 43 age segmentation was performed [14].

3. Methodology

In this section, a methodology for classifying brain tumors is proposed. First, the CNN model flow chart is explained, and then the dataset is preprocessed and augmented. Finally, the SqueezeNet model and the proposed model are discussed in detail.

3.1. CNN model Flow chart

Initially, images will be loaded, and labels will be extracted from datasets files. Then, the dataset is separated into training, validation, and testing sets. The training data will be used to train the network after setting the hyper-parameters. After that, the testing data is applied to the model to test the network. If the accuracy of the model is acceptable. Then, the model is good. If not, we adjust the hyperparameters. As shown in Figure 1.

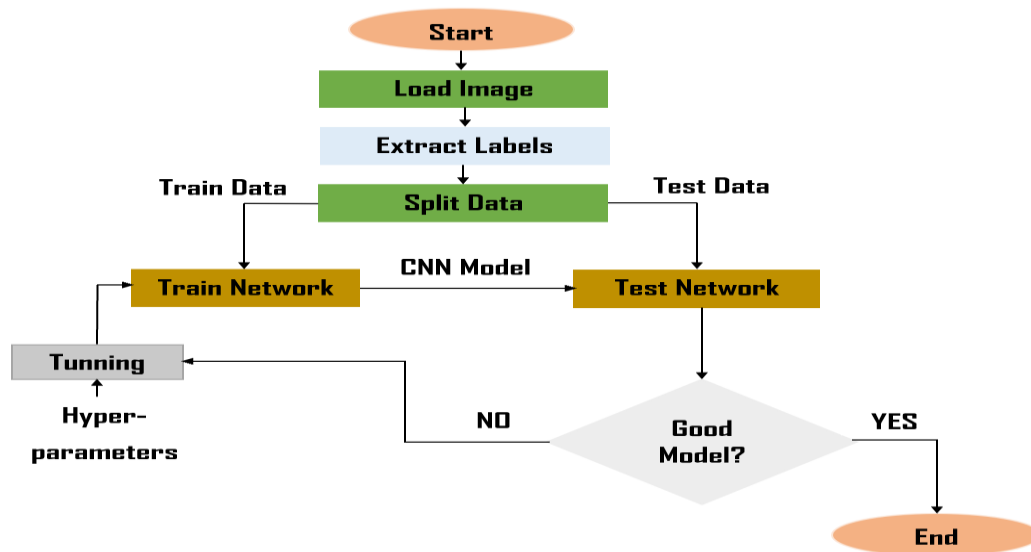


Figure 1. CNN model Flow chart.

3.2 Classification Approach Based on 3DCNN Architecture (Approach [15])

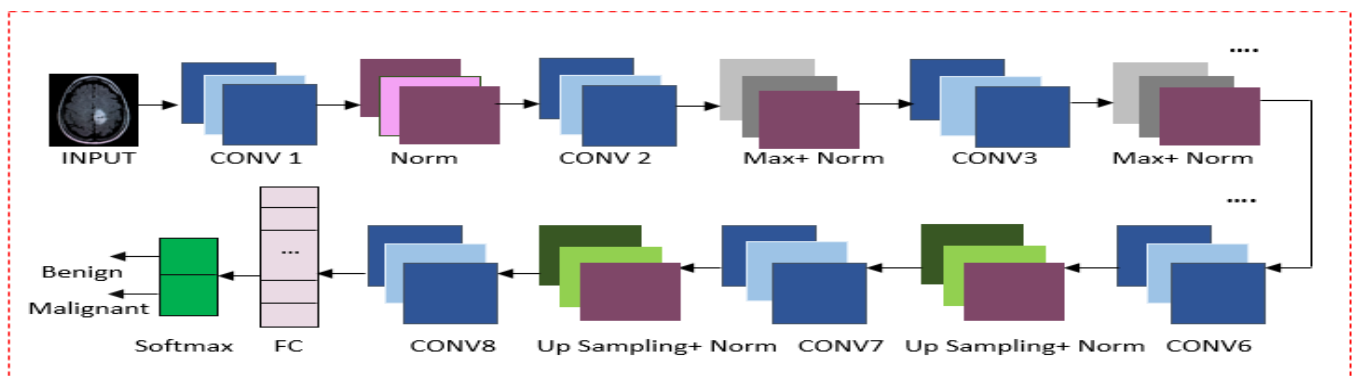


Figure 2. Approach [15] architecture.

This approach contains eight convolutional layers based on 3DCNN [15] and the detailed architecture is illustrated in Figure 2 and Table 1.

Table 1. Proposed [15] Architecture.

| Layer Name | Layer Properties |
|------------|--|
| CONV 1 | 32 3 × 3 × 3 convolutions, stride [2 2 2] |
| CONV 2 | 64 3 × 3 × 3 convolutions, stride [1 1 1] |
| CONV 3 | 128 3 × 3 × 3 convolutions, stride [2 2 2] |
| CONV 4 | 256 3 × 3 × 3 convolutions, stride [1 1 1] |
| CONV 5 | 256 3 × 3 × 3 convolutions, stride [2 2 2] |
| CONV 6 | 128 3 × 3 × 3 convolutions, stride [1 1 1] |
| CONV 7 | 64 3 × 3 × 3 convolutions, stride [2 2 2] |
| CONV 8 | 32 3 × 3 × 3 convolutions, stride [1 1 1] |

3.3 Proposed Approach Based on SqueezeNet Architecture

SqueezeNet is a CNN architecture that achieves the AlexNet accuracy level with 50 fewer parameters [16]. SqueezeNet's basic structure starts with a convolution layer, then eight Fire modules, and finally another convolution layer. Moreover, the max-pooling layer is added after layers Conv1, Fire4, Fire8, and Conv10, ReLU is implemented as the activations function, and 0.5 Dropout is used after the Fire9 module. As shown in Figure 3.

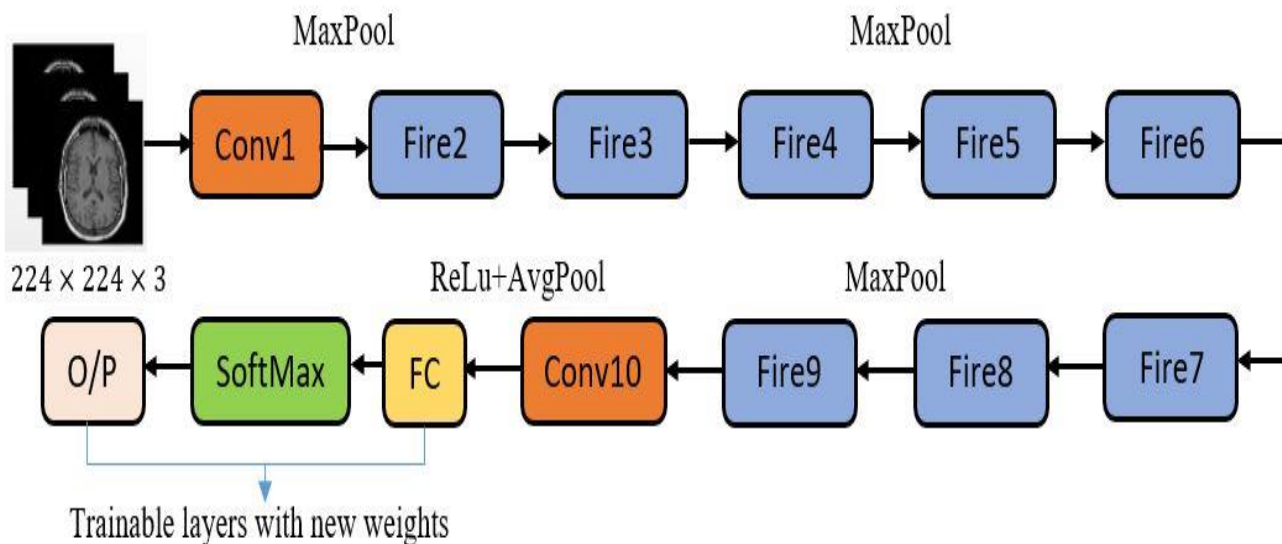


Figure 3. SqueezeNet Architecture.

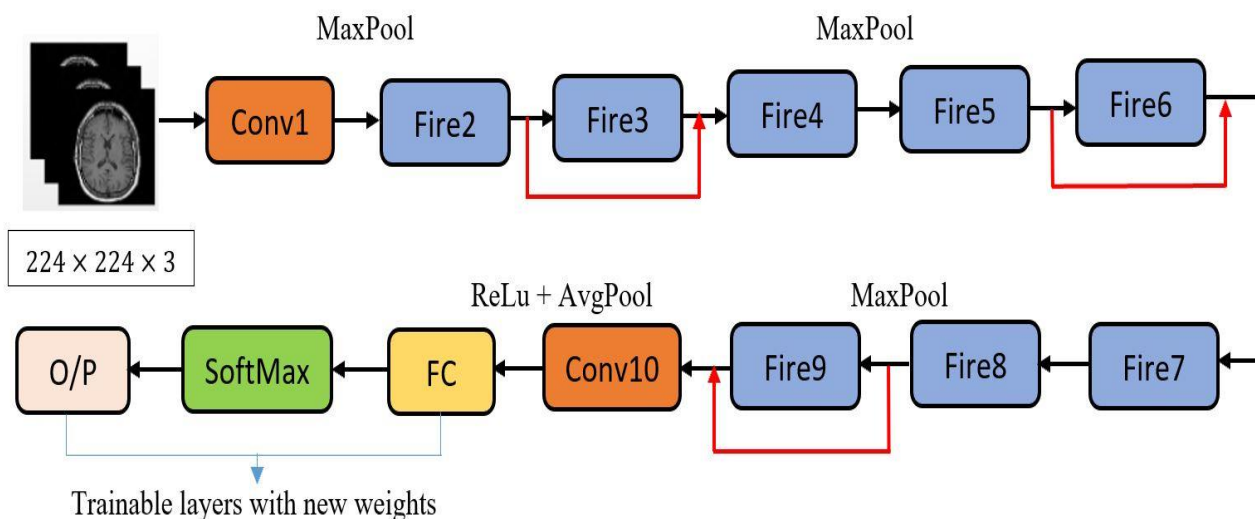


Figure 4. Proposed Approach Architecture.

The proposed approach architecture illustrated in Figure 5 is considered a modified version of SqueezeNet. Where some simple bypass connections have been added between some Fire modules to enhance the recognition accuracy. These connections will be added around Fire modules 3, 6, and 9. Bypass around Fire3, means that the input to Fire4 will be equal to the output of Fire2 + the output of Fire3, where the trigger (+) is added in terms of elements, as shown in Figure 5, and this will change the regulation applied to these Fire module parameters, Thus the model trainability and final accuracy can be improved.

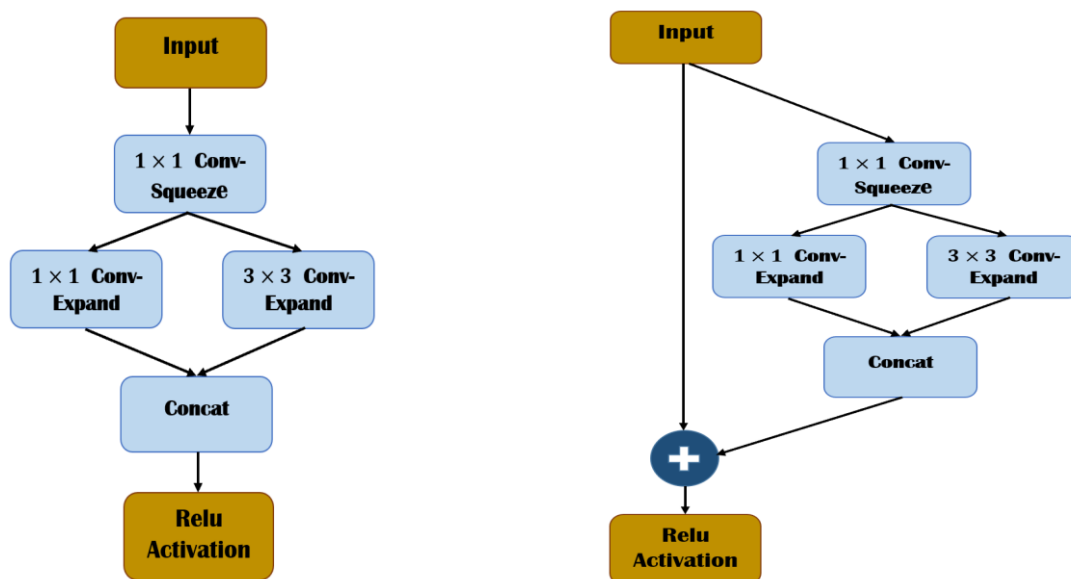


Figure 5. Fire Module Structure: (a) Original Fire Module Structure; (b) Simple bypass Connections of the proposed approach.

The brain tumor detection method algorithm is illustrated below as shown in Figure 6.

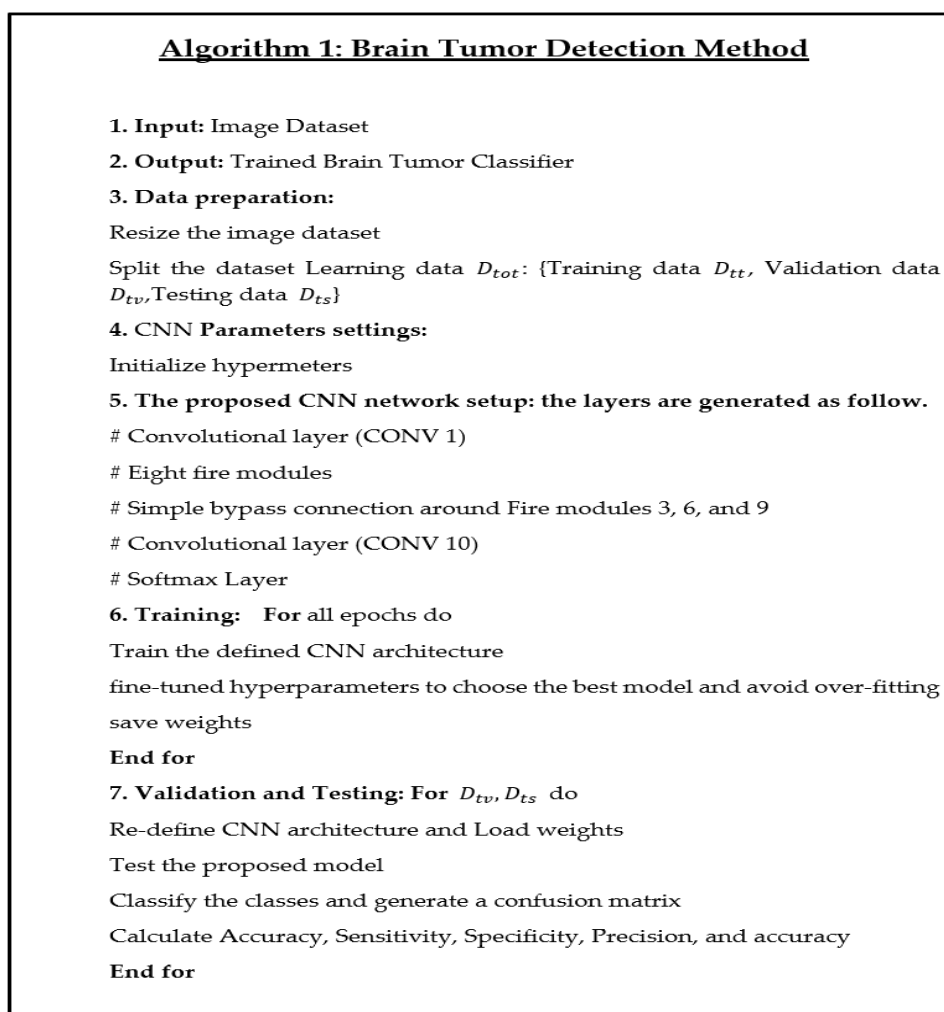


Figure 6. Brain tumor detection algorithm pseudo code.

3.4 Performance Evaluation Metrics Parameters

The measures of Accuracy (ACC.), Specificity (SP.), Precision (PR.), F1-score, and Sensitivity (SN.) metrics [17] are used to evaluate system performance and can be defined as follows.

$$\text{Accuracy} = \frac{TN+TP}{(FN+FP+TN+TP)} \quad (1)$$

$$\text{Specificity} = \frac{TN}{(TN+FP)} \quad (2)$$

$$\text{Precision} = \frac{TP}{(TP+FP)} \quad (3)$$

$$\text{(Sensitivity)Recall} = \frac{TP}{(TP+FN)} \quad (4)$$

$$\text{F1-Score} = 2 \times \frac{\text{Precision} * \text{Recall}}{(\text{Precision} + \text{Recall})} \quad (5)$$

Where TP represents the true positive in the case of malignancy and TN represents the true negative in benign tumor cases, while FP and FN represent the inaccurate model predictions.

4. Results and Discussions

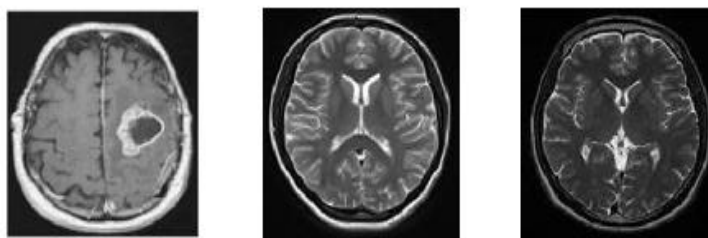


Figure 7. The brain dataset samples for the two classes normal and tumor.

The experiments are carried out on free MRI images classified as normal and tumor [18], which are collected by field experts. 252 MRI samples were obtained from the volunteer patients as illustrated in Table 2. The MRI brain image samples are shown in Figure 7.

Table 2: Dataset Samples

| Brain | Number of MRI images before augmentation | Number of MRI images after augmentation |
|----------|--|---|
| Normal | 126 | 1520 |
| Abnormal | 126 | 1520 |

Because the MRI images in the database are of different formats and sizes. The image resolution is unstable, and its quality is not high. Since these images represent the input layer for the network, they have been resized and normalized to 224×224 pixels. The hyper-parameters used for the simulation process are listed in Table 3.

Table 3: Hyper-parameters of the experiments

| Hyper-parameter | Value |
|------------------------|--------------------|
| Optimization algorithm | SGDM |
| Momentum | 0.9000 |
| Initial learning rate | 1×10^{-4} |
| L2 Regularization | 1×10^{-4} |

Stochastic Gradient Descent with Momentum (SGDM) is the main optimization algorithm because it achieves the desired balance between accuracy and efficiency [19]. But it needs to manipulate the model hyper-parameters, especially the initial learning rate. Since it determines how rapidly weights are adjusted to achieve the smallest loss function.

4.1 Simulation Results

In this subsection, the original dataset will be compared if it is split randomly into 20% for testing and 80% for training and when the splitting ratio is 70:30 (15% for test, 15% validation). Table. 4, shows the performance of the proposed model compared to Approach [15] based on 70:30 and 80:20 splitting ratios.

Table 4: Performance of Proposed model and Approach [15] based on 70:30, 80:20 splitting ratio.

| Split Ratio | Batch Size | Epoch | Proposed Model (Original dataset) Accuracy (%) | Approach [15] Accuracy (%) |
|-------------|------------|-------|--|-------------------------------|
| 80:20 | 32 | 8 | 90.93 | 88.93 |
| | | 9 | 91.65 | 90.88 |
| | | 10 | 93.54 | 92.95 |
| | | 11 | 95.32 | 94.32 |
| | 64 | 8 | 93.69 | 90.69 |
| | | 9 | 95.87 | 94.95 |
| | | 10 | 96.53 | 95.14 |
| | | 11 | 95.83 | 94.83 |
| 70:30 | 32 | 8 | 89.03 | 87.03 |
| | | 9 | 90.41 | 88.64 |
| | | 10 | 92.61 | 90.79 |
| | | 11 | 92.93 | 91.56 |
| | 64 | 8 | 90.42 | 88.32 |
| | | 9 | 92.78 | 90.54 |
| | | 10 | 93.69 | 92.36 |
| | | 11 | 94.86 | 93.90 |

From the previous table, the best accuracy will be achieved when the splitting ratio is 80:20, the batch size is 64 and the number of epochs is 10. Approach [15] attains a maximum accuracy of 95.14%, then the accuracy will be gradually decreased. While the proposed model shows the best result with an accuracy of 96.35%. Then, the network will be overfitted.

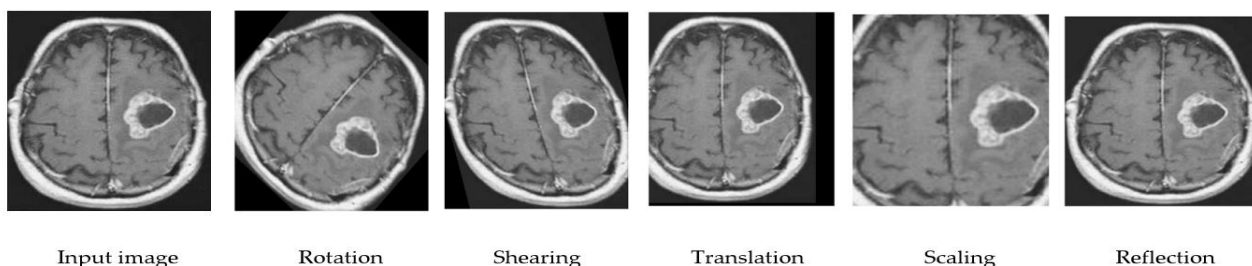
The network training was carried out original dataset (without data augmentation). Whereas the whole brain MRI images were scaled to fit the input image size of each pre-trained DCNN. Table. 5 illustrates the evaluation of performance metrics for the proposed model, approach [15], and other pre-trained models with the original dataset.

Table 5: Performance Evaluation Metrics for the proposed model, and other pre-trained models (splitting ratio 80:20)

| Metrics Algorithm | Accuracy | Precision | Sensitivity | Specificty | F1-score |
|----------------------|----------|-----------|-------------|------------|----------|
| | AlexNet | 86.32 | 90.24 | 83.91 | 90.80 |
| VGG-16 | 83.25 | 88.63 | 80.78 | 86.45 | 82.12 |
| ResNet18 | 92.32 | 93.71 | 90.02 | 93.74 | 91.37 |
| SqueezeNet | 94.23 | 92.81 | 90.53 | 93.75 | 93.81 |
| Approach [15] | 95.14 | 93.55 | 94.12 | 94.77 | 94.91 |
| Proposed Model | 96.35 | 96.12 | 94.22 | 96.23 | 96.3 |

4.2 The Effect of Data augmentation

In this subsection, the effectiveness of data Augmentation will be studied where the classification problem addressed in this paper lacks sufficient data to feed the deep learning architecture and achieves the best accuracy results. Data augmentation techniques increase a training dataset using traditional techniques which generate new data from existing data by applying various transformation techniques such as rotation, scaling, reflection, translation, and shearing as shown in Figure 8.

**Figure 8.** Data augmentation (Image transformation).

The proposed model will be trained using the augmented dataset with the same hyperparameters applied to the original dataset (80:20 splitting ratio, 10 epochs, and 64 batch size).

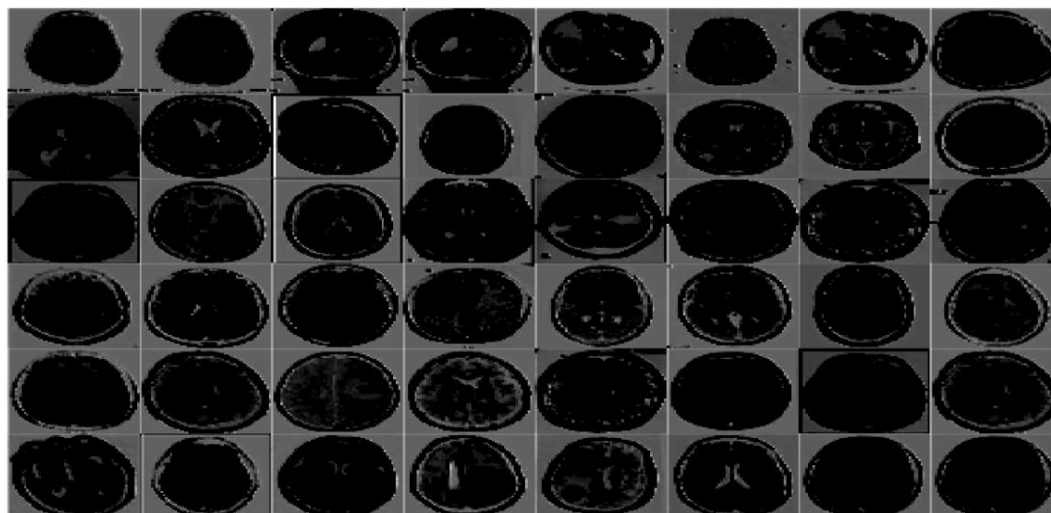
**Figure 9.** Visual representations of output features before the classification layer.

Figure 9 shows the visual representations of some extracted features before the classification layer through the proposed CNN architecture using 48 filters.

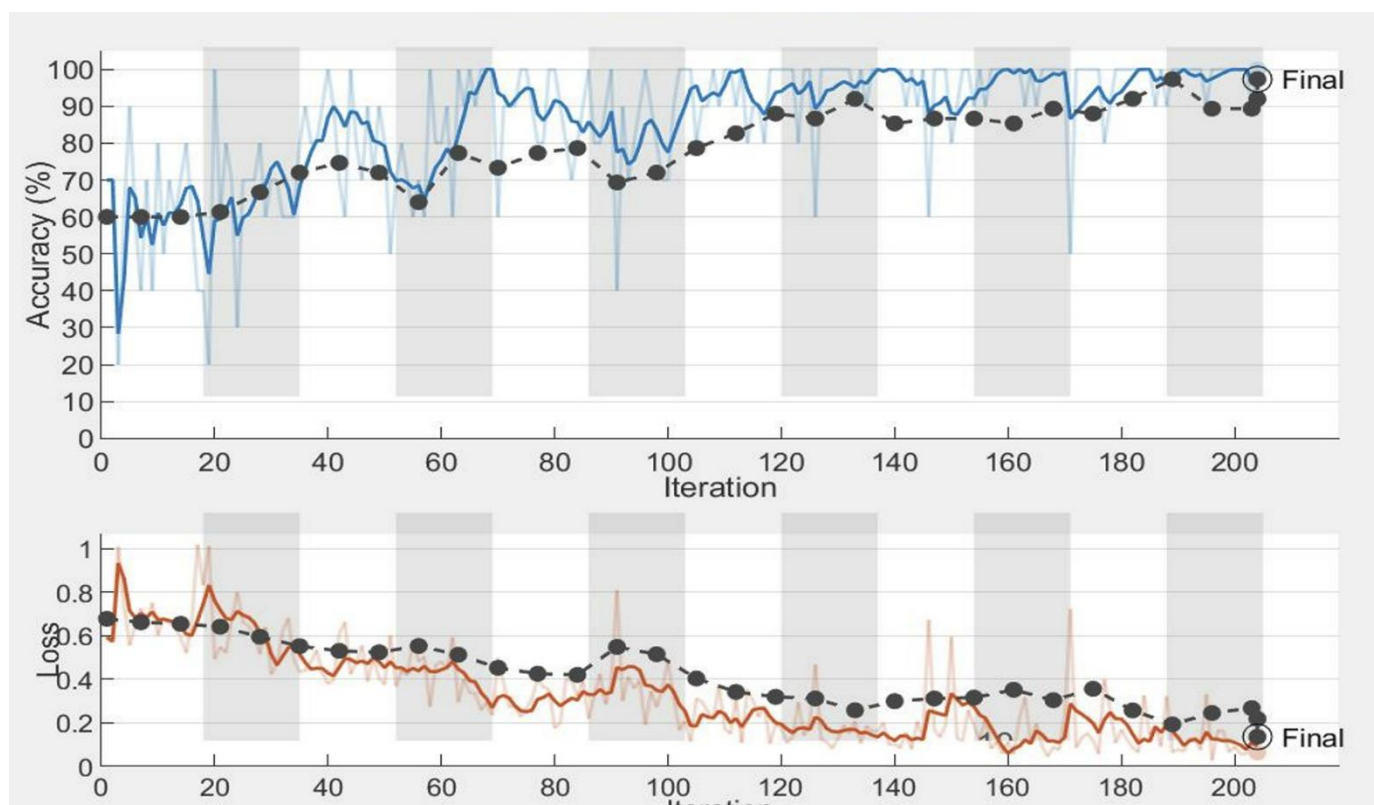


Figure 10. Accuracy and loss curves of the proposed model with 20% for testing and 80% for training in case of the original dataset

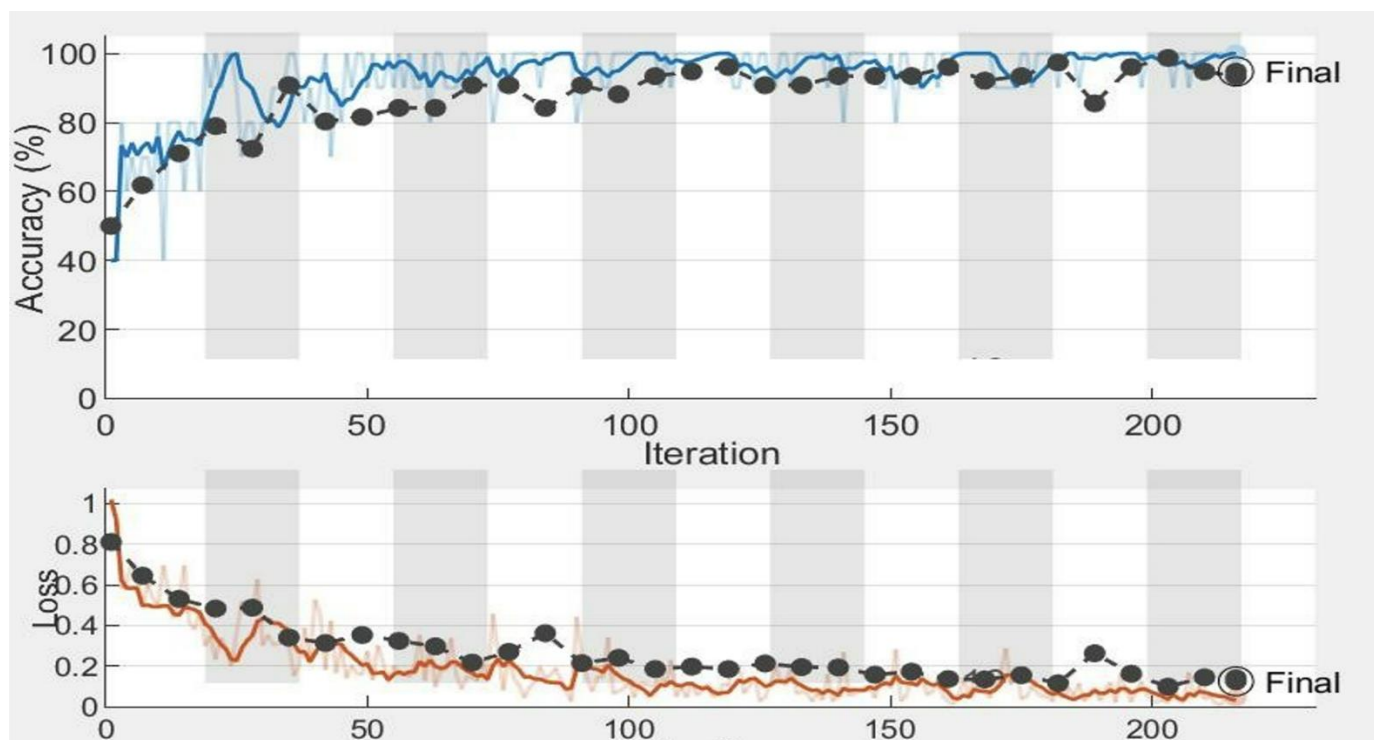


Figure 11. Accuracy and loss curves of the proposed model with 20% for testing and 80% for training in case of the augmented dataset

As shown in Figures (10 and 11), the proposed approach achieves classification accuracies of 96.3%, and 97.78, respectively. when trained by the original dataset, and augmented data, respectively.

For the case of the training CNNs with data augmentation, the approach [15], and our proposed model can achieve better classification performance of 96.62% and 97.78% respectively as shown in Table 6.

Table 6: Performance Evaluation Metrics with Data Augmentation.

| Algorithm | Metrics | | | | |
|----------------|----------|-----------|-------------|-------------|----------|
| | Accuracy | Precision | Sensitivity | Specificity | F1-score |
| AlexNet | 87.83 | 93.06 | 84.35 | 92.22 | 88.42 |
| VGG-16 | 84.48 | 89.54 | 81.32 | 88.41 | 85.26 |
| ResNet18 | 94.86 | 94.2 | 94.40 | 93.93 | 93.62 |
| SqueezeNet | 95.22 | 94.2 | 92.43 | 95 | 94.33 |
| Approach [15] | 96.62 | 95.29 | 96.1 | 95.06 | 95.74 |
| Proposed model | 97.78 | 94.83 | 95.51 | 94.7 | 97.15 |

A confusion matrix is a graph that shows how well a classification network performs on a test dataset where the real values are already known. Figures 12, and 13 demonstrate the matrix of perplexity, which combines the performance of the proposed system in the case of the original dataset and augmented dataset. In the matrix provided, The Target class is shown on the X-axis, while the Output class is shown on the Y-axis. The classification error for the testing set for the proposed model (in the case of original data) is equal to 3.7 %. While the error is 2.3 % in the case of data augmentation for the proposed model.

| | | | | |
|------------|----------|---------------|---------------|-----------------|
| True Class | Normal | 94 37.6% | 4 1.6% | 95.9% 4.1% |
| | Abnormal | 6 2.4% | 146 58.7% | 96.1% 3.9% |
| | | 94.0% 6.0% | 97.3% 2.7% | 96.3% 3.7% |
| | | Normal | Abnormal | Predicted Class |

Figure 12. Confusion matrix of the proposed model (in the case of original data).

| | | | | |
|------------|----------|------------------------|-----------------|---------------|
| True Class | Normal | 96 38.7% | 0 0.0% | 100% 0.0% |
| | Abnormal | 4 1.6% | 150 60.0% | 97.4% 2.6% |
| | | 96.0% 4.0% | 100% 0.0% | 97.7% 2.3% |
| | | Normal | Abnormal | |
| | | Predicted Class | | |

Figure 13. Confusion matrix of the proposed model (in the case of data augmentation).

4.3 Performance Evaluation Comparison Study

The classification results obtained from the proposed model and approach [15] are represented as a graphical comparison shown in Figure 14. Where the results with data augmentation are all better in terms of accuracy than the ones without data augmentation.

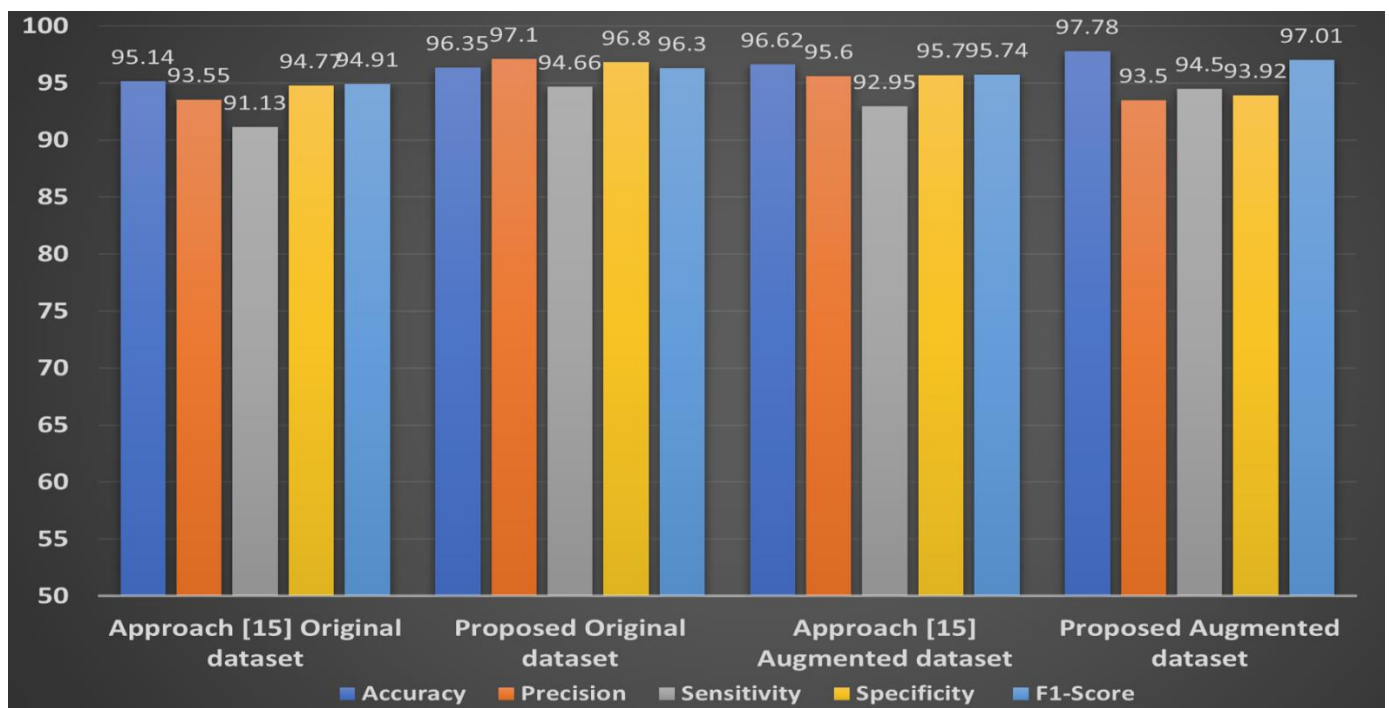


Figure 14. Performance measures for Approach [15] and proposed with (Original dataset, Augmented dataset).

Figure 15 illustrates the accuracy of the proposed model in the case of data augmentation obtained during the testing phase with a value of 97.78% which is reached after 130 iterations with the number of epochs equal to 10, and a learning rate of 0.0001.

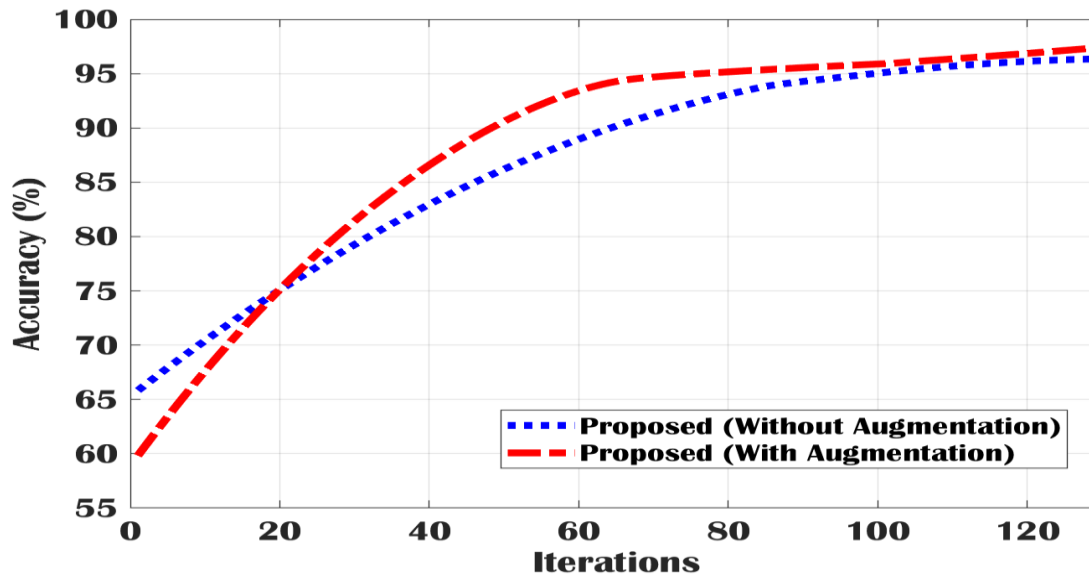


Figure 15. Results over the whole training iterations for the proposed model: Accuracy curve.

The loss value reduces gradually with the increase in the number of iterations, as illustrated in Figure 16. The suggested model's loss curve is assigned a value less than its value for the original dataset when the dataset is augmented.

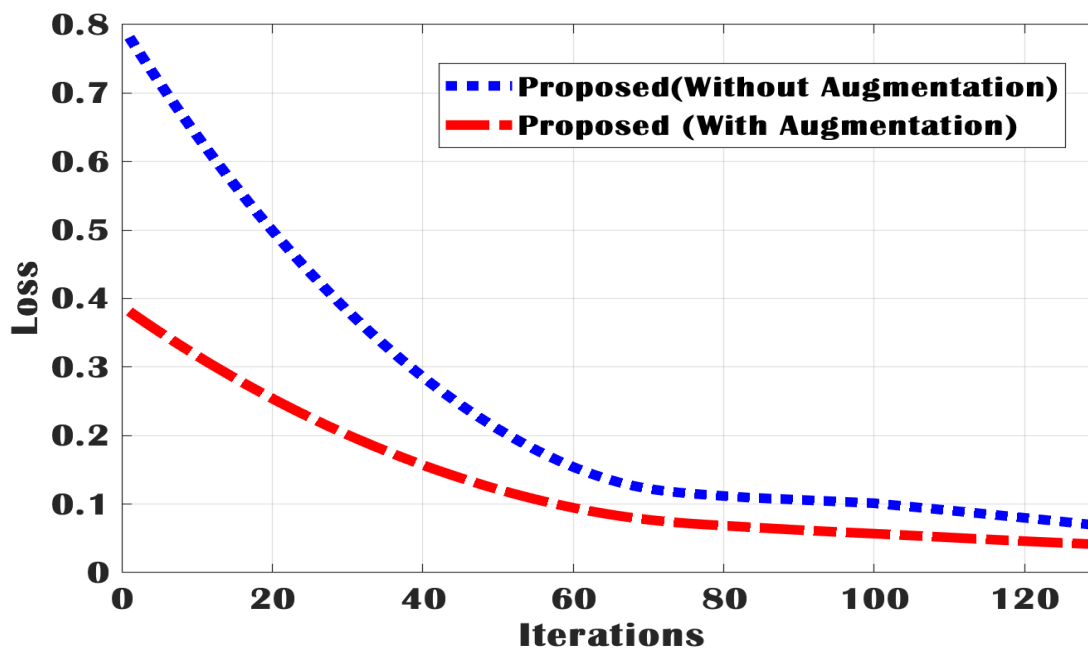


Figure 16. Results over the whole training iterations for the proposed model: Loss curve.

The processing time is an important consideration when evaluating the proposed system's performance. Table 7 shows the average processing time for the proposed approach compared with other pretrained models.

Our model's average training time per epoch is 110 seconds, compared to 245 seconds for the VGG-16, 151 seconds for AlexNet, 261 seconds for squeezeNet, and 398 seconds for ResNet 18. As a result, our model requires fewer computational specifications because it runs faster compared to other pretrained models. Furthermore, our model outperforms VGG-16, AlexNet, ResNet 18, and squeezeNet in terms of accuracy.

Table 7: Average training time of the proposed model with pre-trained models (in case of data augmentation).

| Algorithm | No. of layers | Training time | Accuracy |
|----------------|---------------|---------------|----------|
| AlexNet | 25 | 30 min 13 sec | 87.83 |
| VGG-16 | 41 | 48 min 50 sec | 84.48 |
| ResNet 18 | 71 | 79 min 42 sec | 94.86 |
| SqueezeNet | 68 | 52 min 21 sec | 95.22 |
| Proposed Model | 68 | 22 min 8 sec | 97.78 |

The ROC curve for the suggested model is shown in Figure 17. The proposed model with data augmentation has achieved an AUC value of 97.7%. Meanwhile, the original dataset shows an AUC value of 96.3%.

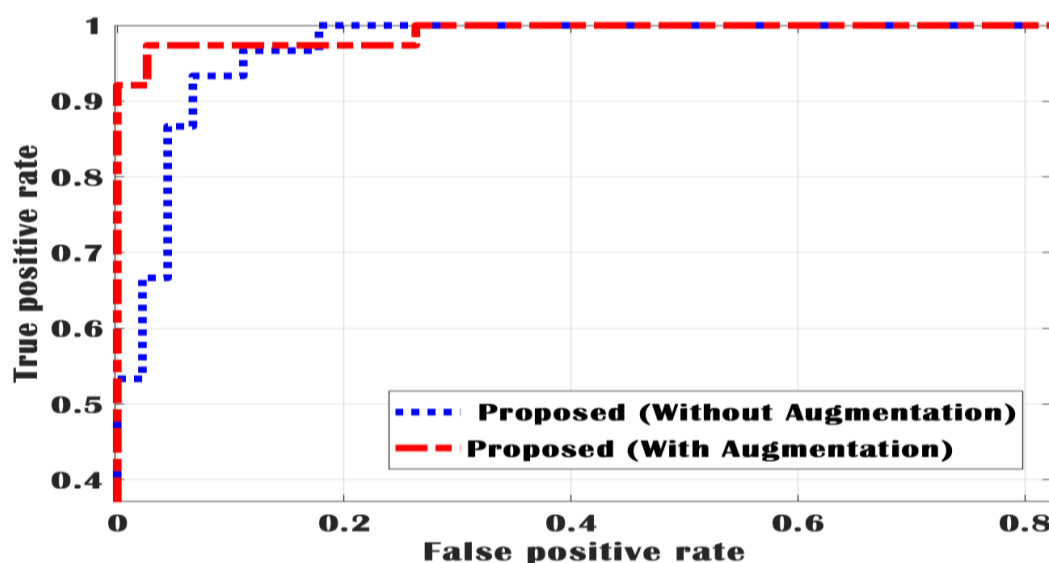


Figure 17. Receiving Operating Characteristic (ROC) Curve of the proposed model.

The proposed approach must be compared to results from the literature review to determine the reliability and validity of the obtained results. The outcome of the proposed solution is shown in Table 8.

Table 8: Different studies on brain tumor detection techniques.

| Approach | Classifier | Dataset | Accuracy (%) |
|-----------------|------------|---------------------------------|--------------|
| Ref [19] | CNN | 253 images | 95 |
| Ref [20] | CNN | 220 images | 94.5 |
| Ref [21] | PSO+SVM | 612 images | 97.4 |
| Ref [22] | CNN | 3064 images | 97.3 |
| Ref [23] | CNN | 253 images | 97.2 |
| Proposed Method | CNN | 252 images (Original Dataset) | 96.53 |
| Proposed Method | CNN | 1500 images (Augmented dataset) | 97.78 |

5. Conclusions

Among the millions of cancerous diseases, brain tumor is the critical one. According to research, the global number of brain tumors cases is growing. Any damage to the brain can directly lead to death. As a result, early diagnosis and treatment of these diseases are critical. Because speed and time are crucial considerations.

This paper presents a deep learning model based on CNN for the classification of brain tumor MR images into the normal and abnormal brain. The network has been trained using the original data with a splitting ratio of 80:20 and achieves an accuracy of 96.3%. Moreover, the impact of augmenting the dataset has been discussed, the proposed model attains an accuracy of 97.78% at the augmented data is split to the same ratio. Finally, a comparative study between the suggested model and other models has been made in terms of accuracy, precision, specificity, sensitivity, and F1-score.

Conflicts of Interest: “The authors declare no conflict of interest.”

References

1. NHS, National Health Service: Brain Tumours, 2020. Available from: <https://www.nhs.uk/conditions/brain-tumours/>.
2. Cancer. Net, Brain Tumor: Statistics, 2020. Available from: <https://www.cancer.net/cancer-types/brain-tumor/statistics>
3. Fu GS, LS. YH. Machine Learning for Medical Imaging. *Journal of Healthcare Engineering*, 1-2, 2019.
4. Ronneberger O, Fischer P, Brox. U-Net: Convolutional networks for biomedical image segmentation. *Medical Image Computing and Computer-Assisted Intervention MICCAI*, 234-241, 2015.
5. Andersson EBR. Evaluation of Data Augmentation of MR Images for Deep Learning. Available online <https://lup.lub.lu.se/student-papers/search/publication/8952747>. (Accessed on 09 March 2019).
6. S. Basheera, M. S. S. Ram, Classification of brain tumors using deep features extracted using CNN. *J. Phys.* 1172, 2019.
7. R. Carlo, C. Renato, C. Giuseppe, U. Lorenzo, I. Giovanni, S. Domenico, Distinguishing Functional from Non-functional Pituitary Macroadenomas with a Machine Learning Analysis. *Mediterranean Conference on Medical and Biological Engineering and Computing*, Springer. 1822–1829, 2019.
8. M. Sajjad, S. Khan, M. Khan, W. Wu, A. Ullah, S. W. Baik, Multi-grade brain tumor classification using deep CNN with extensive data augmentation. *J. Comput. Sci.* 30, 174–182, 2019.
9. S. Das, R. Aranya, N. Labiba. Brain tumor classification using a convolutional neural network. 2019 1st International Conference on Advances in Science, Engineering and Robotics Technology (ICASERT), 10, 2019.
10. V. Romeo, R. Cuocolo, C. Ricciardi, L. Uggia, S. Coccozza, F. Verde, et al. Prediction of tumor grade and nodal status in oropharyngeal and oral cavity squamous-cell carcinoma using a radiomic approach, *Anticancer Res.*, 40, 271–280, 2020.
11. M. Talo, U. B. Baloglu, O. Yildirim, U. R. Acharya, Application of deep transfer learning for automated brain abnormality classification using MRI images, *Cognitive Systems Research*, 54, 176–188, 2019
12. A. Rehman, S. Naz, M. I. Razzak, F. Akram, M. Imran, A Deep Learning-Based Framework for Automatic Brain Tumors Classification Using Transfer Learning. *Circuits Syst. Signal Process.*, 39, 757–775, 2020.
13. A. Cinar, M. Yildirim, Detection of tumors on brain MRI images using the hybrid convolutional neural network architecture. *Med. Hypotheses*, 139, 2020.
14. Banerjee, Subhashis, et al. Glioma classification using deep radiomics. *SN Computer Science*, 1-14, 2020
15. S. A. El-Feshawy, W. Saad, M. Shokair, and M. Dessouky. Brain Tumour Classification Based on Deep Convolutional Neural Networks. *International Conference on Electronic Engineering (ICEEM)*, 1-5, 2021.
16. R. C. Patil, and A. S. Bhalchandra. Brain tumor extraction from MRI images using MATLAB,” *International Journal of Electronics. Communication and Soft Computing Science & Engineering (IJECSCE)*, 2012.
17. Comert, Z., Sengur, A., Budak, U., Kocamaz, AF. Prediction of intrapartum fetal hypoxia considering feature selection algorithms and machine learning models.
18. Chakrabarty N. Brain MRI Images for Brain Tumor Detection | Kaggle n.d. Available online: <https://www.kaggle.com/navoneel/brain-mri-images-for-brain-tumor-detection> (Accessed on 10 June 2019)
19. P. Saxena, A. Maheshwari, and S. Maheshwari. Predictive modeling of brain tumor: A deep learning approach. *Innovations in Computational Intelligence and Computer Vision*, 275–285, 2021.
20. Hemanth, D.J.; Anitha, J.; Naaji, A.; Geman, O.; Popescu, D.E. A modified deep convolutional neural network for abnormal brain image classification. *IEEE Access*, 7, 4275–4283, 2018.
21. Gudigar, A., Raghavendra, U., San, T. R., Ciaccio, E. J., & Acharya, U. R. Application of multiresolution analysis for automated detection of brain abnormality using MR images: A comparative study. *Future Generation Computer Systems*, 90, 359-367, 2019.
22. Francisco, J.P.; Mario, Z.M.; Miriam, R.A. A Deep Learning Approach for Brain Tumor Classification and Segmentation Using a Multiscale Convolutional Neural Network. *Healthcare*, 9, 153, 2020.
23. A. Cinar and M. Yildirim, “Detection of tumors on brain mri images using the hybrid convolutional neural network architecture,” *Medical hypotheses*, 139, 2020.